Materials Characterization 217 (2024) 114314

Contents lists available at ScienceDirect

Materials Characterization

journal homepage: www.elsevier.com/locate/matchar

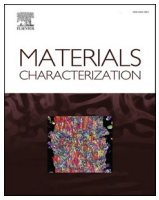

Measuring the twinning stress at the micron scale: A comprehensive comparison of testing geometries

Camila Aguiar Teixeira, Subin Lee *, Christoph Kirchlechner

Institute for Applied Materials, Karlsruhe Institute of Technology, D-76131 Karlsruhe, Germany

ARTICLE INFO

Keywords:
Deformation twinning
In situ micro mechanical testing
micro-pillar compression
micro-cantilever bending
micro-shear test
High entropy alloys

ABSTRACT

Three micro mechanical testing geometries including micro-pillars, micro-cantilevers and micro-shear specimen, were employed to measure the twinning stress of the Cantor high entropy alloy. This study presents a comparative analysis of the challenges in specimen preparation, effectiveness in activating deformation twinning and complexity of *post mortem* analyses associated with each geometry. Our findings demonstrate that micro-shear testing represents the optimal approach for twinning studies, offering direct activation of the twinning system with the superior reproducibility compared to other geometries. Micro-pillar compression is also suitable for twinning investigations, providing statistical analysis of mechanical data with relatively faster sample preparation. However, micro-cantilever testing presents challenges with a lower success rate in twinning activation and the stress gradients, which complicates quantitative interpretation, resulting in the least favorable geometry for twinning studies.

1. Introduction

Outstanding mechanical properties have shaped the Cantor alloy, and its derivatives, into the most studied high entropy alloys (HEAs) thus far [1–5]. Deformation twinning plays an important role in their mechanical behavior, especially under cryogenic temperatures contributing to an increase in tensile strength and ductility [4–7]. The extensive mechanical twinning observed is attributed to their low stacking fault energy, which is reported to range from 20 to 35 $mJ \bullet m^{-2}$ [8–13]. It is well-established that twin boundaries may act as barriers to dislocation motion dynamically, which delays necking instability and rupture providing additional ductility [6]. In room temperature, dislocation slip is dominant, as the lower tensile stresses require higher strains for twinning activation, by work hardening, only being observed close to fracture [6]. Therefore, twinning is envisioned to be a stress-controlled mechanism and this particular stress that should be reached for its nucleation is known as the twinning stress [14]. Deformation twinning is often attributed to improvement of mechanical properties, consequently, comprehensive understanding of the mechanism, also quantitatively (*i.e.* measuring twinning stress), is crucial for development of not only HEAs but also new advanced alloys.

There have been attempts to experimentally measure twinning stress in the Cantor alloy in respect to effects of stacking fault energy, temperature, grain size and orientation [6,8,9,12,13,15]. The experimental work typically involves interrupted macro-scale tests, followed by *post mortem* analyses using techniques such as electron backscatter diffraction (EBSD) or transmission electron microscopy (TEM) to confirm the activation of twinning. However, such measurements performed on macroscopic polycrystals may fail to provide the twinning stress quantitatively, as local stress depends on the local microstructure and resulting stress heterogeneities. To explore the mechanical behavior in the micro to nanoscale and gain quantitative understanding of mechanisms, focused ion beam (FIB)-based *in situ* micro mechanical testing was developed [16]. This technique allows for measuring mechanical properties locally and, therefore, to target specific grains or grain boundaries, while simultaneously observing the deformation behavior, finally enabling the investigation of underlying mechanisms individually [17].

In situ scanning electron microscope (SEM) micro mechanical testing has been applied to study deformation twinning of FCC alloys, but only, to the authors' knowledge, on TWIP steels and CoCrNiFe HEA using micro-pillar compression [18–23]. Besides typical micro-pillar compression, other established micro mechanical geometries, for instance micro tensile or shear tests, are suited to study twinning mechanism and measure twinning stress maintaining a uniaxial stress distribution. Micro-pillar testing generally suffers from experimental

* Corresponding author.
E-mail address: subin.lee@kit.edu (S. Lee).

https://doi.org/10.1016/j.matchar.2024.114314
Received 14 June 2024; Received in revised form 26 August 2024; Accepted 28 August 2024
Available online 6 September 2024

limitations, including non-uniform stress distribution due to tapering, friction between indenter tip and top surface, sample buckling leading to aspect ratio limitation, and compliance issues [17,24,25]. Micro-tensile experiments offer an alternative; the ability to fabricate samples with higher aspect ratios reduces experimental constrains as in micro-pillar application [26]. However, sample fabrication is relatively time-consuming which so far has restrained this geometry from wider use [17]. Alternatively, micro-cantilevers could be considered for mechanical testing. Fabricating a cantilever is faster than a tensile specimen and, additionally, this geometry allows to explore anisotropy with introduction of both tensile and compressive stresses, however, the stress gradient can complicate quantitative interpretation of mechanical data considerably. Another relatively unexplored uniaxial test is micro-shear testing which has been successfully applied on a few occasions in the micro mechanical field [27–30]. The advantage of this geometry is that it can directly activate the desired slip system, by applying pure shear on {111} planes, with no contrains, allowing free dislocation glide [27,28].

Therefore, this study aims to investigate and compare three different micro mechanical geometries with different stress states, and determine which is the most suitable for twinning stress measurements and mechanism studies based on effectiveness, sample preparation and *post mortem* analyses. A comparison between micro-shear, cantilever and pillar tests are conducted. By choosing a geometry dependent grain orientation, the resolved shear stress will be maximized on the leading partial dislocation favoring twin nucleation in each geometry.

2. Materials and methods

2.1. Fabrication of alloy

The equiatomic CoCrFeMnNi alloy was prepared with high purity elements (99.95 + %) on an arc melting furnace under Ar atmosphere. After the melting process, the sample was cast as rod-shaped ingots in a water-cooled Cu mold. The sample composition measured by an inductively coupled plasma optical emission spectrometry was: 20.4 at. % Co, 19.7 at.% Cr, 20.3 at.% Fe, 19.2 at.% Mn and 20.4 at.% Ni (accuracy of 0.1 at.%) [31]. The as-cast material underwent homogenization in a glass tube at 1473 K for 72 h followed by water quenching. A reduction of diameter, from 14 mm to 6 mm, was performed by rotary swaging. Subsequently the sample was annealed at 1273 K for 1 h obtaining a fully recrystallized microstructure with a grain size of approximately 60 μm. A more detailed description of the fabrication process can be found in references [31, 32]. TEM bright-field investigations confirmed a low dislocation density for the annealed sample [32]. Pieces, 1 mm thick, were cut with a diamond saw and metallographical prepared to obtain a deformation free surface. Sample surface preparation consisted in grinding up to 2500 mesh and polishing with firstly diamond suspension of 3 μm and 1 μm, and finished with oxide polishing suspension (0.02 μm particle size).

2.2. Fabrication and testing of micro specimens

2.2.1. Micro-shear testing

Micro-shear specimens shown in Fig. 1(a) require a precise alignment of the sample geometry with respect to the crystallographic orientation in both, the in-plane and the loading directions. The in-plane alignment, more specifically the ligament-normal direction, should correspond to the twinning plane, {111}, while the loading direction should be aligned to the twinning direction ⟨112⟩ to maximize shear stress in the ligament thus activate deformation twinning. Therefore, crystallographic orientation analysis was done using EBSD (Symmetry S2, Oxford Instruments) at acceleration voltage of 20 kV and a current of 8 nA in FIB-SEM (Crossbeam 550 L, Zeiss). Once the [112] (surface-normal direction) grain was chosen and correctly aligned with $(11\bar{1})$ plane in transverse direction (TD), a large cut was performed with

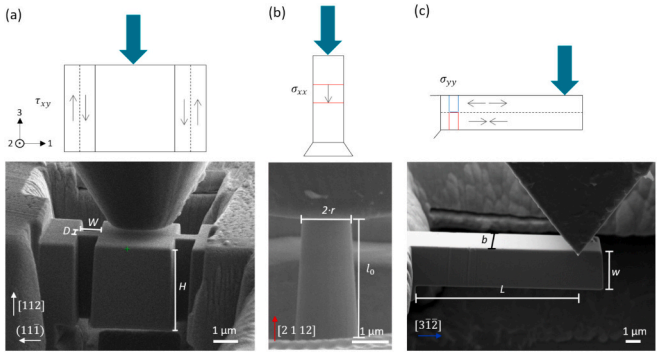

Fig. 1. Micro mechanical geometries applied to measure twinning stress and their corresponding cross-section view with internal stress state represented by arrows: (a) micro-shear, (b) micro-pillar compression and (c) micro-cantilever bending test.

femtosecond laser ablation, also in the same Zeiss Crossbeam 550 L to expose the grain desired for milling from side. Specimens were then micro machined using the FIB with an acceleration voltage of 30 kV and currents starting with 3 nA for coarse, 700 pA for intermediate and 50 pA for fine milling. Sample dimensions were based on literature [28,29] keeping the same aspect ratio with $D = 500$ nm, $W = 750$ nm, and $H = 3$ μm. *In situ* deformation tests were performed in an SEM (Merlin Gemini II, Zeiss) with a Hysitron PI89 NG SEM Picoindenter (Bruker) with a load transducer with maximum force of 0.5 N and noise floor of 5 μN, equipped with a 2 μm diamond flat punch tip (Synthon-MDP AG). All tests were conducted in a displacement control mode with a shear strain rate of $1.33 \times 10^{-2}\ s^{-1}$. Engineering shear stress (τ) and strain (γ) were calculated according to equations respectively:

$$\tau_0 = P/2{\cdot}H{\cdot}D \tag{1}$$

$$\gamma = \Delta/W \tag{2}$$

where P is the load and Δ is the displacement applied, W is the width, D is the thickness and H is the height of the shear ligaments.

2.2.2. Micro-pillar testing

In FCC crystals, deformation twinning activation under compression is expected in near a ⟨001⟩ orientation, where resolved shear stress is maximized on the leading partial dislocation. Therefore, EBSD analysis was performed in the same FIB-SEM with the setting as mentioned in section 2.2.1. Micro-pillars with diameters of 0.5 μm and 1 μm (1:2–3 diameter-height aspect ratio) were micromachined in grains with [2 1 12] and [1 1 10] normal orientation, respectively, using the same FIB at 30 kV and varying milling steps. For 1 μm micro-pillars, currents started with 7 nA for coarse, 1.5 nA for intermediate and 300 pA for fine milling. And for the 0.5 μm micro-pillars, currents starting with 1.5 nA for coarse, 700 pA for intermediate and 50 pA for fine milling were used. *In situ* SEM testing was performed with the same indenter used for the micro-shear experiments. Two different transducers were used for each diameter; one mentioned in section 2.2.1 was used for the 1 μm micro-pillars, and another transducer with maximum load of 10 mN and noise floor 0.4 μN was used for the 0.5 μm micro-pillars. The indenter was equipped with a 2 μm diamond flat punch tip and micro-pillar compressions were done in a displacement-controlled mode with $10^{-2}\ s^{-1}$ strain rate. To calculate the engineering stress (σ) and strain (ε) the following equations were considered:

$$\sigma = P/\pi r^2 \tag{3}$$

$$\varepsilon = \Delta l/l_o \tag{4}$$

where P is the load and Δl the displacement applied, l_0 is the initial height and r the top radius of the micro-pillar (Fig. 1(b)).

2.2.3. Micro-cantilever testing

EBSD was performed (similarly to described on section 2.2.1 and 2.2.2.) to select a grain with a TD near a ⟨111⟩, which favors deformation twinning under tensile stresses. Five cantilevers were prepared from three different grains of which TD orientation is $[3\bar{1}\bar{2}]$, $[\bar{1}32]$ and $[11\bar{1}]$, respectively. As shown in Fig. 1(c), micro-cantilevers with dimensions of $W = b = 2$ μm and $L = 10$ μm were then micro machined in the same FIB operated at 30 kV using ion beam currents of 3 nA for coarse, 700 pA for intermediate and 50 pA for fine milling. *In situ* deformation test was performed in a SEM (Merlin Gemini II, Zeiss) with a Hysitron PI89 NG SEM Picoindenter (Bruker) with a 10 μm diamond wedge tip (Synthon-MDP AG) using displacement-controlled mode and a displacement rate of 10 nm/s. For the micro-cantilever stress (σ) calculations the fully plastic case was assumed (schematically shown in Fig. 1(c)), which is calculated by the equation:

$$\sigma = 4 \cdot P \cdot L / b \cdot W^2 \quad (5)$$

where P is the applied load, L is the length, b the width and W the thickness of the cantilever.

3. Results

3.1. Micro-shear testing

Micro-shear testing in general is a unique technique from a mechanical and physical point of view, considering that it is not only a simple case of multiaxial loading condition ($\sigma_1 = -\sigma_3 \neq 0, \sigma_2 = 0$), but also enables activation of a specific slip system by pure shear [28]. As seen in Fig. 1(a), during the test the flat punch tip compresses the central loading block which, if well aligned, slides parallel to the {111} plane and causes activation of the desired slip system by pure shear. In this work's specific case, the micro-shear geometry is implemented to activate deformation twinning, which has a {111} twinning plane and a ⟨112⟩ twinning direction. Therefore, the sample in Fig. 1 is aligned with the $(11\bar{1})$ plane on the in-plane TD and the [112] twinning loading direction.

An experimental overview of the micro-shear test and a representative engineering shear stress *versus* strain curve are shown with the corresponding to *post mortem* SEM image (Fig. 2(a) and (b)). After elastic deformation, the shear stress reached a plateau of around 300 MPa, which is slightly higher than the twinning stress reported in literature, around 240 MPa [6,33]. The average plateau stress or critical resolved shear stress (CRSS) for twinning from four samples is 339 ± 16 MPa. Note that throughout the manuscript, the mean value of all tested samples and the standard deviation are provided. Shear sliding on the $(11\bar{1})$ plane parallel to the loading direction is observed, suggesting a good in-plane alignment, as well as a slight indentation impression, which indicates some plastic deformation on the center loading block prior to sliding of both ligaments (Fig. 2(b)).

Then, EBSD analysis on both shear ligaments was performed to identify deformation twinning. Note that "L" and "R" labels each ligament on Fig. 2(b) and 2(c). 1.5 μm thick of top layer was removed by FIB to guarantee a flat top surface and avoid possible shadowing on the EBSD detector. As a result, nanoscale twin lamellas were observed in the shear region "L", highlighted by the red arrows on the inverse pole figure (IPF)-Z shown in Fig. 2(c), which was confirmed by both misorientation of 60 degrees and [111] pole figures from the twinned lamella and the matrix which share one common pole which corresponds to the twin plane. For sheared region "R" no twin microstructure was observed with EBSD analysis, which could be explained by opposing shear crystallographic directions in each ligament as shown in Fig. 2(b). Contrary to deformation slip, twinning is polarized which means that opposing twinning direction will no longer trigger twin formation due to similar reasons for tension-compression asymmetry in deformation twinning [34]. Therefore, the imposed shear direction in one of the sheared regions will always be contrary to twin formation.

The contribution of deformation twinning to overall shear strain can be estimated with the micro-shear geometry. This contribution was calculated with: (i) the twin displacement computed by the known crystallographic orientation relation between twin and matrix, and measured twin thickness (from EBSD IPF-Z maps); (ii) divided by the total displacement of each micro-shear specimen. The total displacement applied was in average 851.59 nm, and the shear displacement introduced by twinning was in average 18.20 nm, which corresponds to

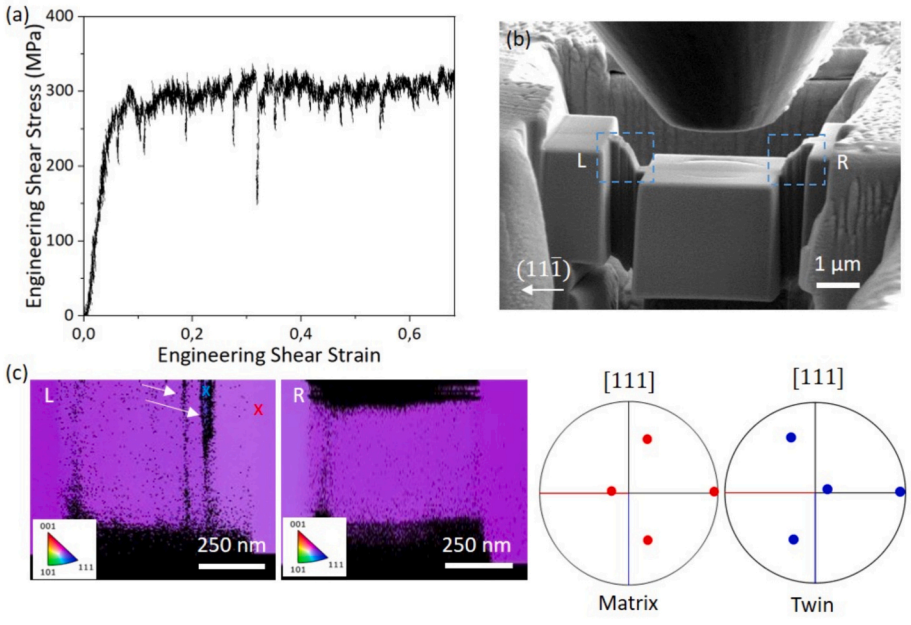

Fig. 2. Micro-shear test representative engineering shear stress and shear strain curve (a), *post mortem* SEM image (b), EBSD inverse pole figure (IPF-Z) (c) in regions "L" and "R" and [111] pole figures from twinned lamella and matrix (the red arrows on the IPF-Z highlights the twin lamella). Note that the blue (twin lamella) and red (matrix) "x" on the IPF-Z indicates the positions the pole figures were considered. (For interpretation of the references to colour in this figure legend, the reader is referred to the web version of this article.)

2.13 % of overall shear strain. It should be noted that this contribution provides only the lower bound due the resolution limit of EBSD which could be unable to resolve possible nanoscale twin lamellas formed. However, it is clear that the majority of the shear deformation is introduced by dislocation slip and twinning has only a small contribution.

3.2. Micro-pillar compression

Under compressive stress state, as represented in Fig. 1(b), deformation twinning activation in FCC is favored near a ⟨001⟩ crystallographic orientation. In this case, the highest Schmid factor is for leading partial dislocations, consequently the resolved shear stress increases the separation width between two partial dislocations and promotes deformation twinning [19,20]. To compare the results with the other micro mechanical geometries tested, two different micro-pillar diameters (0.5 μm and 1 μm) were tested and in each case 3 samples.

One of the advantages of micropillar compression is easier interpretation of the mechanical data as the raw load-displacement curve can be easily converted to an engineering stress-strain curve as shown in Fig. 3(a) which is representative for 1 μm micro-pillars. Since the micro-pillars were fabricated in a grain with a normal orientation near ⟨001⟩ which 8 possible slip systems have similar Schmid factor, activation of more than one slip system is likely to happen (Fig. 3(b)). In multiple slip activation conditions, slip direction identification *via post mortem* SEM analysis is challenging, but the slip planes observed were analyzed to as $(\bar{1}11)$ and $(1\bar{1}1)$. In both slip plane cases, only one slip direction under compression can trigger deformation twinning that would result on the slip systems of $(\bar{1}11)[\bar{1}1\bar{2}]$ and $(1\bar{1}1)[1\bar{1}2]$. Further *post mortem* analyses with EBSD of the micro-pillar top surface and cross-section imaging with the backscattered electron (BSE) detector, Fig. 3(c) and 3(d) respectively, identified a twin formed on the $(\bar{1}11)$ slip plane and consequently the $[\bar{1}1\bar{2}]$ twinning direction. Afterwards, CRSS is calculated as 294 ± 46 MPa based on the slip analysis which results in the Schmid factor for the activated twinning system of 0.46, and the yield stress taken with a 2 % offset. For the micro-pillars with reduced diameter of 0.5 μm, the CRSS calculated was 425 ± 197 MPa. A higher CRSS compared to the literature values [6,33] and larger scatter of the data can be explained by mechanical size-effects, expected in small scale, that leads to a stochastic behavior [17].

3.3. Micro-cantilever bending

For the micro-cantilever bending test, 3 samples in ⟨123⟩ and 2 samples in $[11\bar{1}]$ TD, in other words the long cantilever axis, were tested. Therefore, under tensile stresses two distinct conditions are expected: on (i) ⟨123⟩ orientations a single slip system is expected with a higher Schmid factor for the leading partial dislocation; and on (ii) $[11\bar{1}]$ is a multi-slip system orientation resulting in 6 possible slip systems to be activated and 3 possible twinning directions.

Figure 4(a) shows a representative load-displacement curve and Fig. 4(b) is its respective *post mortem* image for the cantilevers with $[3\bar{1}\bar{2}]$ TD. In this single slip orientation only slip systems on the $(11\bar{1})$ plane was expected to be activated due to the highest Schmid factor, on $[1\bar{1}0]$ full slip direction of 0.46 or on $[\bar{1}21]$ twinning direction of 0.47. However, as shown in the SEM *post mortem* image (Fig. 4(b)), two slip planes were activated: $(11\bar{1})$ and $(1\bar{1}\bar{1})$. For this specific case, a 3.5 μm displacement was applied, most likely increasing strain concentration near the cantilever base and consequently leading to activation of a secondary slip system. Further EBSD analyses, seen in Fig. 4(c), have identified a twinned microstructure in the $(1\bar{1}\bar{1})$ slip plane with the $[\bar{1}21]$ twinning direction and a Schmid factor of 0.30, which results in a CRSS of 237 MPa assuming a pure tensile stress in the cantilever in fully plastic condition.

However, for the other two cantilevers tested in the $[\bar{1}32]$ TD

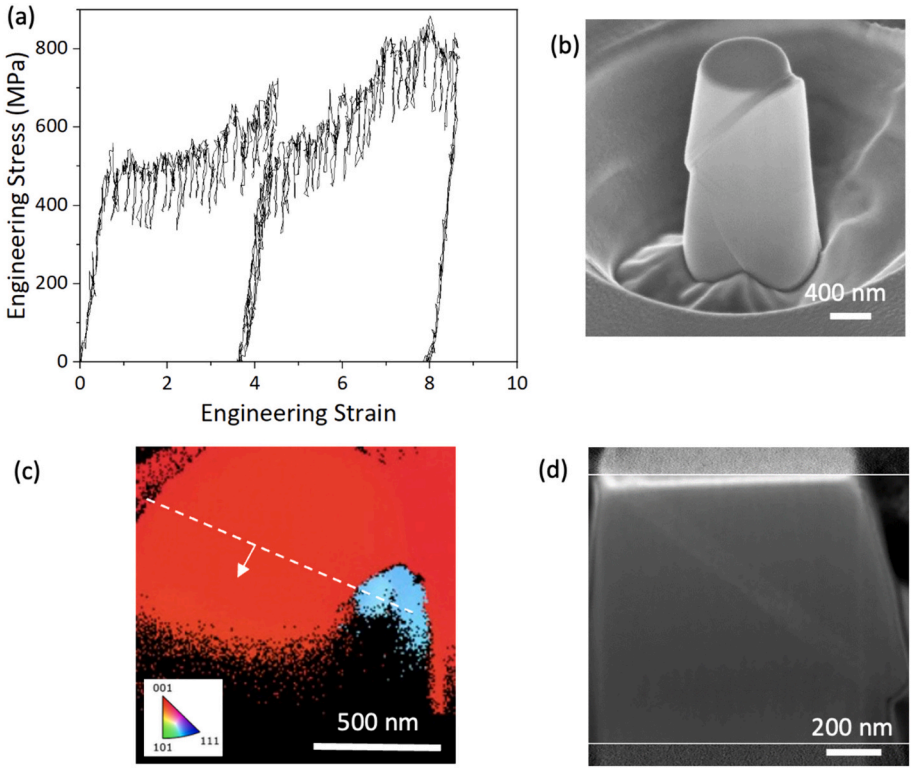

Fig. 3. Representative engineering stress and strain curve (a) of a 1 μm diameter micro-pillar compression test and corresponding *post mortem* SEM image (b). EBSD IPF-Z analysis (c) on the micro-pillar's top surface and cross section SEM imaging (d). Cross section viewing direction is highlighted by white dashed line and arrow on EBSD IPF-Z (c).

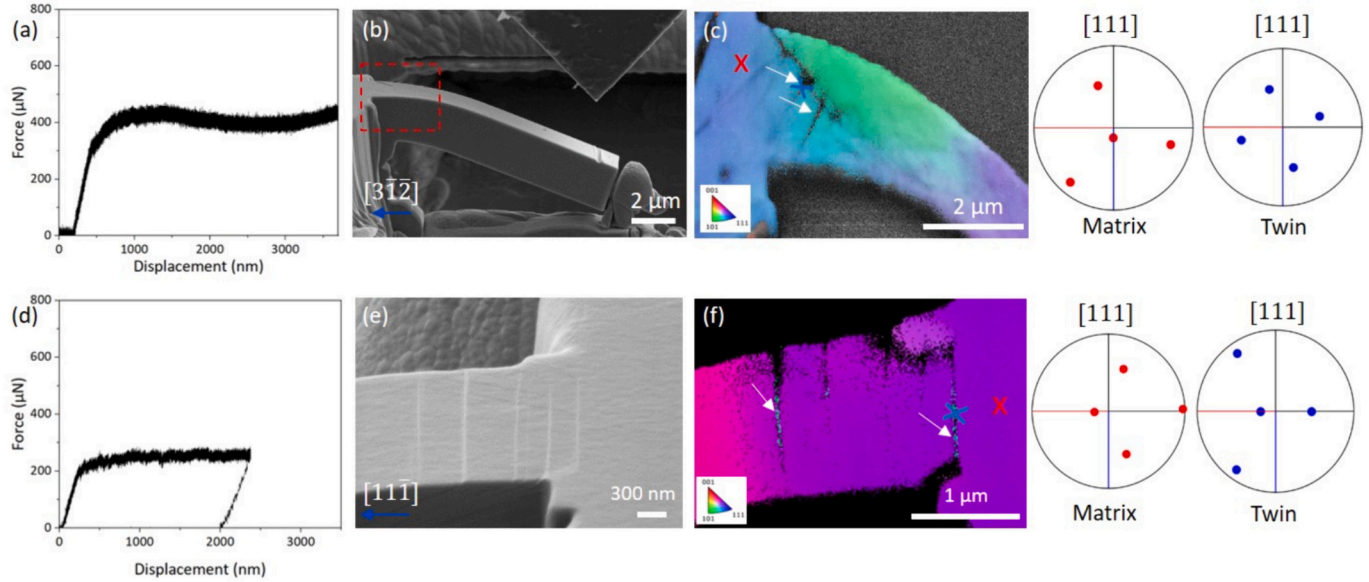

Fig. 4. Micro-cantilever bending force and displacement curves for samples of [3$\bar{1}\bar{2}$] (a) and [11$\bar{1}$] (d) TD orientation. Corresponding *post mortem* SEM images of sample [3$\bar{1}\bar{2}$] (b) and [11$\bar{1}$] (e) (red dashed rectangle in (b) highlights the region EBSD analysis was performed). EBSD IPF-Z analyses (white arrows pointing to the twin lamella) and [111] pole figure of twin and matrix is shown in (c) for [3$\bar{1}\bar{2}$] and in (f) for [11$\bar{1}$]. Note that the blue (twin lamella) and red (matrix) "x" on the IPF-Z indicates the positions the pole figures were considered. (For interpretation of the references to colour in this figure legend, the reader is referred to the web version of this article.)

orientation, no deformation twinning could be observed with EBSD analyses. In this case, SEM *post mortem* imaging identified only slip on the (1$\bar{1}$1) planes and no secondary slip was triggered during deformation. It is important to point out that there was a difference in the maximum displacement applied, ranging from 0.5 to 1 μm each. According to the slip analyses, the (1$\bar{1}$1)[110] slip system was activated during the test, with a Schmid factor of 0.46.

In the case of the 2 samples on the [11$\bar{1}$] TD orientation (Fig. 4(d)–(f)), as expected, multiple slip systems were activated. *Post mortem* SEM imaging analyses showed two slip planes activated for one sample and all three possible ones for the other. Note that the samples were arranged within the same grain similarly to [$\bar{1}$32] TD orientation ones. They were loaded to a maximum displacements of 1 μm and 2 μm each. As seen in Fig. 4(e), three slip planes were observed on the cantilever with largest displacement (2 μm). EBSD analyses (Fig. 4(f)) were carried out and twin microstructure could only be observed in the cantilever with largest displacement on the (111) slip plane and [11$\bar{2}$] twinning direction with a Schmid factor of 0.31. For the full slip case the Schmid factor is 0.27. This resulted in an average of 301 ± 63 MPa for samples which activated deformation twinning and 292 ± 26 MPa for samples that did not.

Assuming twinning as a stress-controlled mechanism, those results could be considered as conflicting once comparing cantilevers of same orientation and respective reached stresses. Which leads to believe that, under bending, additional criteria need to be met for twinning nucleation. For instance, deformation twinning was only observed in cantilevers with the largest displacement applied, from 2 to 3.5 μm, thus it seems that a particular stress concentration near the cantilever base is required, and it was not reached in some cases. Additionally, the absence of twinning could also be explained similarly to the micro-shear experiments, which would hold true for one cantilever in both [11$\bar{1}$] and [$\bar{1}$32] orientations. For each direction, the two cantilevers were arranged one in front of the other, hence the bending moment sign is opposite in each case, which favors twinning in one case but suppresses it in the other. Therefore, even if the required stresses were reached, twinning could only be formed in one of the directions and, once the moment sign is reversed, it can no longer occur.

4. Discussion

4.1. Comparison between testing geometries

In this work, three different micro mechanical geometries with different stress states during deformation were applied to study deformation twinning and measure twinning stress. Deformation twinning was successfully activated in all geometries, however, each presented challenges in terms of preparation, *post mortem* analyses and geometry efficiency that will be discussed and compared in this section.

The micro-shear geometry could be considered as the optimal approach for deformation twinning studies. This geometry enables direct activation of the twinning system without constraints, allowing free dislocation glide and with comparably low resolved shear stress for competing dislocation mechanisms (*e.g.* slip on other slip systems). In terms of quantitative mechanical data, results have shown the smallest standard deviation indicating good reproducibility compared to the other geometries, as seen in Fig. 5, which compares twinning stresses measured from each geometry. Hence micro-shear testing does not require many tests for a meaningful statistical conclusion. In addition, *post mortem* analysis was relatively straightforward; after removing the top layer by FIB side-milling to provide a flat surface, EBSD analysis was easily performed, and the twin microstructure was observed in all tested samples. However, as previously stated, several factors should be considered when applying this geometry for deformation twinning studies. Perfect alignment with {111} slip planes is required to activate a specific slip system, otherwise any misalignments could result in additional slip system activation. Additionally, it can be time-consuming; for instance, in polycrystalline samples, a large material removal might be required to expose the desired grain for the study, adding to the complexity of working with this geometry. Also, since twinning is polarized, it will only be activated in one of the shear regions due to opposite shear direction in respect to twinning direction, which may result in asymmetric loading.

Some of the drawbacks associated with the micro-shear testing such as alignment challenges, time-consuming fabrication and twinning direction issues for activation can be address by micro-pillar compression. Among the geometries tested, micro-pillars are by far the fastest to

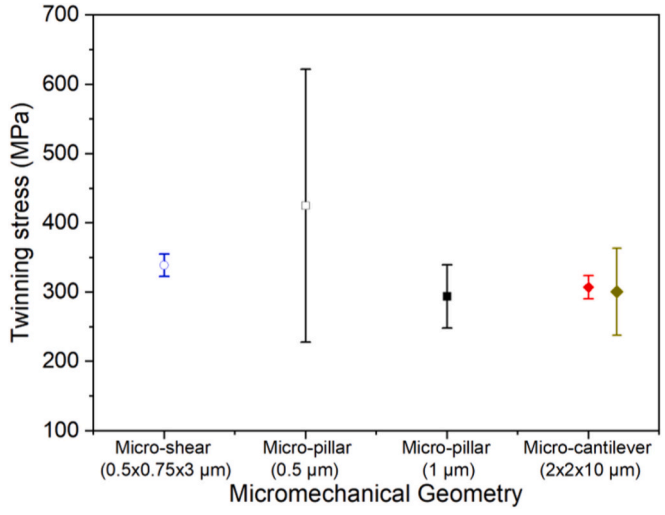

Fig. 5. Comparative plot of CRSS and respective micro mechanical geometry. Note that each geometry is represented by a shape (*e.g.* micro-pillars represented by a square) and stresses are compared according to samples dimension. In the micro-cantilever case, red markers represent the sample that deformation twinning was not activated and yellow markers the sample that did. (For interpretation of the references to colour in this figure legend, the reader is referred to the web version of this article.)

fabricate with easiest crystallographic alignment, since only the normal orientation needs to be considered which can be quickly analyzed using EBSD. Then, micro-pillars can rapidly be milled with annular milling techniques, which allows statistical data analyses. The mechanical data, as seen in Fig. 5, in average was consistent with the other geometries within the same dimensions, although it presents a large deviation as expected in a micro to nanoscale testing and already discussed in section 3.2. Micro-pillar *post mortem* analyses, however, can be challenging particularly when the formed twin lamella are nanoscale, which might not be resolved in an EBSD scan performed at the top surface and may require further lift-out and TEM investigations. Please note that similar challenges may arise with other geometries. Nevertheless, micro-pillar compression is a unique tool for size effect studies, as it enables mechanical tests in a micro to nanoscale and provides important insights into underlying mechanisms. Therefore, micro-pillar is a suitable geometry to measure the twinning stress and investigate twinning mechanisms.

In the micro-cantilever case, investigating deformation twinning and measuring twinning stress is more complex compared to the other geometries. Sample fabrication can be as tedious as the micro-shear specimens in terms of milling time and TD alignment, considering a polycrystalline bulk sample. In the experimental test set up, contrary to a flat punch tip, the wedge tip requires a good alignment with the micro-cantilever to avoid activating unexpected slip systems. Results have also shown that, under bending, there seems to be additional criteria besides stresses reached and TD for twinning activation. The mechanical data was consistent with micro-pillars of similar dimension, as seen in Fig. 5, but only 2 out of 5 samples activated deformation twinning. As discussed in section 3.3, a careful analysis of the bending moment and twinning direction, or larger displacements might be necessary to promote deformation twinning. Finally, tensile stresses may be easier to apply through micro-cantilever bending test, rather than time-consuming micro tensile experiments, however, it is no longer a uniaxial stress distribution, and the strain gradient complicates data interpretation and correlation to the twinning mechanism.

5. Conclusions

Three different micro mechanical geometries have been applied to investigate and measure the twinning stress of the Cantor alloy. In summary:

- Micro-shear tests represent the optimal conditions for mechanical twinning activation with superior reproducibility compared to the other geometries. This geometry allows for clear discrimination between twinning and dislocation slip. However, due to the opposite shearing direction in each of shear region, twinning can only be nucleated on one side.
- Micro-pillar compression is a suitable geometry for twinning stress measurements and mechanism studies, particularly because of its ease to be applied. Overall, it showed an average mechanical data consistent with other geometries within same dimensions, coupled with fast and uncomplicated crystallographic alignment for sample preparation. However, due to mechanical size effect a large number of micro-pillars should be tested to obtain a meaningful mechanical data and the twin lamella formed, once nanoscale, may require extensive *post mortem* analyses.
- Micro-cantilever has shown to be the least suitable geometry to measure twinning stress, considering that twinning was only activated in 2 out 5 samples tested and due to stress gradient the correlation of stresses and deformation mechanism is complex.

CRediT authorship contribution statement

Camila Aguiar Teixeira: Writing – original draft, Visualization, Methodology, Investigation, Formal analysis, Data curation, Conceptualization. **Subin Lee:** Writing – review & editing, Supervision, Methodology, Investigation, Formal analysis, Data curation, Conceptualization. **Christoph Kirchlechner:** Writing – review & editing, Supervision, Methodology, Funding acquisition, Formal analysis, Conceptualization.

Declaration of competing interest

The authors declare that they have no known competing financial interests or personal relationships that could have appeared to influence the work reported in this paper.

Data availability

Data can be made available upon reasonable request.

Acknowledgments

The authors gratefully acknowledge the Robert Bosch Stiftung and Helmholtz Program Materials Systems Engineering for their financial support. Reinhard Pippan, Guillaume Laplanche, Jon Molina and Ujjval Bansal are gratefully acknowledged for the fruitful scientific discussions. Alexander Kauffmann is gratefully acknowledged for providing the samples for this work. The Karlsruhe House of Young Scientist (KHYS) is gratefully acknowledged for the Networking Grant granted and Jon Molina for kindly accepting the hosting period in IMDEA.

References

[1] D.B. Miracle, O.N. Senkov, A critical review of high entropy alloys and related concepts, Acta Mater. 122 (2017) 448–511, https://doi.org/10.1016/j.actamat.2016.08.081.
[2] E.P. George, W.A. Curtin, C.C. Tasan, High entropy alloys: a focused review of mechanical properties and deformation mechanisms, Acta Mater. 188 (2020) 435–474, https://doi.org/10.1016/j.actamat.2019.12.015.
[3] E.P. George, D. Raabe, R.O. Ritchie, High-entropy alloys, Nat. Rev. Mater. 4 (2019) 515–534, https://doi.org/10.1038/s41578-019-0121-4.
[4] B. Gludovatz, A. Hohenwarter, K.V.S. Thurston, H. Bei, Z. Wu, E.P. George, R. O. Ritchie, Exceptional damage-tolerance of a medium-entropy alloy CrCoNi at cryogenic temperatures, Nat. Commun. 7 (2016) 1–8, https://doi.org/10.1038/ncomms10602.

[5] B. Gludovatz, A. Hohenwarter, D. Catoor, E.H. Chang, E.P. George, R.O. Ritchie, A fracture-resistant high-entropy alloy for cryogenic applications, Science 345 (2014) 1153–1158, https://doi.org/10.1126/science.1254581.
[6] G. Laplanche, A. Kostka, O.M. Horst, G. Eggeler, E.P. George, Microstructure evolution and critical stress for twinning in the CrMnFeCoNi high-entropy alloy, Acta Mater. 118 (2016) 152–163, https://doi.org/10.1016/j.actamat.2016.07.038.
[7] G. Laplanche, A. Kostka, C. Reinhart, J. Hunfeld, G. Eggeler, E.P. George, Reasons for the superior mechanical properties of medium-entropy CrCoNi compared to high-entropy CrMnFeCoNi, Acta Mater. 128 (2017) 292–303, https://doi.org/10.1016/j.actamat.2017.02.036.
[8] C. Wagner, G. Laplanche, Effect of grain size on critical twinning stress and work hardening behavior in the equiatomic CrMnFeCoNi high-entropy alloy, Int. J. Plast. 166 (2023) 103651, https://doi.org/10.1016/j.ijplas.2023.103651.
[9] C. Wagner, G. Laplanche, Effects of stacking fault energy and temperature on grain boundary strengthening, intrinsic lattice strength and deformation mechanisms in CrMnFeCoNi high-entropy alloys with different Cr/Ni ratios, Acta Mater. 244 (2023) 118541, https://doi.org/10.1016/j.actamat.2022.118541.
[10] N.L. Okamoto, S. Fujimoto, Y. Kambara, M. Kawamura, Z.M.T. Chen, H. Matsunoshita, K. Tanaka, H. Inui, E.P. George, Size effect, critical resolved shear stress, stacking fault energy, and solid solution strengthening in the CrMnFeCoNi high-entropy alloy, Sci. Rep. 6 (2016) 1–10, https://doi.org/10.1038/srep35863.
[11] S.F. Liu, Y. Wu, H.T. Wang, J.Y. He, J.B. Liu, C.X. Chen, X.J. Liu, H. Wang, Z.P. Lu, Stacking fault energy of face-centered-cubic high entropy alloys, Intermetallics 93 (2018) 269–273, https://doi.org/10.1016/j.intermet.2017.10.004.
[12] I.V. Kireeva, Y.I. Chumlyakov, Z.V. Pobedennaya, I.V. Kuksgausen, I. Karaman, Orientation dependence of twinning in single crystalline CoCrFeMnNi high-entropy alloy, Mater. Sci. Eng. A 705 (2017) 176–181, https://doi.org/10.1016/j.msea.2017.08.065.
[13] M. Kawamura, M. Asakura, N.L. Okamoto, K. Kishida, H. Inui, E.P. George, Plastic deformation of single crystals of the equiatomic Cr−Mn−Fe−co−Ni high-entropy alloy in tension and compression from 10 K to 1273 K, Acta Mater. 203 (2021), https://doi.org/10.1016/j.actamat.2020.10.073.
[14] R.E. Kubilay, W.A. Curtin, Theory of twin strengthening in fcc high entropy alloys, Acta Mater. 216 (2021) 117119, https://doi.org/10.1016/j.actamat.2021.117119.
[15] W. Abuzaid, H. Sehitoglu, Critical resolved shear stress for slip and twin nucleation in single crystalline FeNiCoCrMn high entropy alloy, Mater. Charact. 129 (2017) 288–299, https://doi.org/10.1016/j.matchar.2017.05.014.
[16] M.D. Uchic, D.M. Dimiduk, J.N. Florando, W.D. Nix, Sample dimensions influence strength and crystal plasticity, Science 305 (2004) 986–989, https://doi.org/10.1126/science.1098993.
[17] G. Dehm, B.N. Jaya, R. Raghavan, C. Kirchlechner, Overview on micro- and nanomechanical testing: new insights in interface plasticity and fracture at small length scales, Acta Mater. 142 (2018) 248–282, https://doi.org/10.1016/j.actamat.2017.06.019.
[18] S.Z. Wu, H.W. Yen, M.X. Huang, A.H.W. Ngan, Deformation twinning in submicron and micron pillars of twinning-induced plasticity steel, Scr. Mater. 67 (2012) 641–644, https://doi.org/10.1016/j.scriptamat.2012.07.023.
[19] W.S. Choi, S. Sandlöbes, N.V. Malyar, C. Kirchlechner, S. Korte-Kerzel, G. Dehm, B. C. De Cooman, D. Raabe, Dislocation interaction and twinning-induced plasticity in face-centered cubic Fe-Mn-C micro-pillars, Acta Mater. 132 (2017) 162–173, https://doi.org/10.1016/j.actamat.2017.04.043.
[20] W.S. Choi, B.C. De Cooman, S. Sandlöbes, D. Raabe, Size and orientation effects in partial dislocation-mediated deformation of twinning-induced plasticity steel micro-pillars, Acta Mater. 98 (2015) 391–404, https://doi.org/10.1016/j.actamat.2015.06.065.
[21] Z.Y. Liang, J.T.M. De Hosson, M.X. Huang, Size effect on deformation twinning in face-centred cubic single crystals: experiments and modelling, Acta Mater. 129 (2017) 1–10, https://doi.org/10.1016/j.actamat.2017.02.063.
[22] Z.Y. Liang, M.X. Huang, Deformation twinning in small-sized face-centred cubic single crystals: experiments and modelling, J. Mech. Phys. Solids 85 (2015) 128–142, https://doi.org/10.1016/j.jmps.2015.09.004.
[23] Q. Zhang, R. Huang, J. Jiang, T. Cao, Y. Zeng, J. Li, Y. Xue, X. Li, Size effects and plastic deformation mechanisms in single-crystalline CoCrFeNi micro/nanopillars, J. Mech. Phys. Solids 162 (2022) 104853, https://doi.org/10.1016/j.jmps.2022.104853.
[24] D. Kiener, C. Motz, G. Dehm, Micro-compression testing : a critical discussion of experimental constraints, Mater. Sci. Eng. A 505 (2009) 79–87, https://doi.org/10.1016/j.msea.2009.01.005.
[25] C. Kirchlechner, J. Keckes, C. Motz, W. Grosinger, M.W. Kapp, J.S. Micha, O. Ulrich, G. Dehm, Impact of instrumental constraints and imperfections on the dislocation structure in micron-sized cu compression pillars, Acta Mater. 59 (2011) 5618–5626, https://doi.org/10.1016/j.actamat.2011.05.037.
[26] D. Kiener, W. Grosinger, G. Dehm, R. Pippan, A further step towards an understanding of size-dependent crystal plasticity: in situ tension experiments of miniaturized single-crystal copper samples, Acta Mater. 56 (2008) 580–592, https://doi.org/10.1016/j.actamat.2007.10.015.
[27] J. Pfetzing-Micklich, S. Brinckmann, S.R. Dey, F. Otto, A. Hartmaier, G. Eggeler, Micro-shear deformation of pure copper, Materwiss, Werksttech 42 (2011) 219–223, https://doi.org/10.1002/mawe.201100715.
[28] J.K. Heyer, S. Brinckmann, J. Pfetzing-Micklich, G. Eggeler, Microshear deformation of gold single crystals, Acta Mater. 62 (2014) 225–238, https://doi.org/10.1016/j.actamat.2013.10.002.
[29] M. Seok, H. Gopalan, S. Nandy, S. Zaefferer, D. Raabe, C. Kirchlechner, G. Dehm, Microscale plastic anisotropy of basal and pyramidal I slip in pure magnesium tested in shear, Materialia 14 (2020) 100932, https://doi.org/10.1016/j.mtla.2020.100932.
[30] C.M. Lauener, F. Schwarz, L. Pethö, J.M. Wheeler, J. Michler, R. Spolenak, Orientation-dependent extreme shear strain in single-crystalline silicon - from elasticity to fracture, Mater. Des. 235 (2023) 112423, https://doi.org/10.1016/j.matdes.2023.112423.
[31] A.S. Tirunilai, J. Sas, K.P. Weiss, H. Chen, D.V. Szabó, S. Schlabach, S. Haas, D. Geissler, J. Freudenberger, M. Heilmaier, A. Kauffmann, Peculiarities of deformation of CoCrFeMnNi at cryogenic temperatures, J. Mater. Res. 33 (2018) 3287–3300, https://doi.org/10.1557/jmr.2018.252.
[32] K. Lu, A. Chauhan, A.S. Tirunilai, J. Freudenberger, A. Kauffmann, M. Heilmaier, J. Aktaa, Deformation mechanisms of CoCrFeMnNi high-entropy alloy under low-cycle-fatigue loading, Acta Mater. 215 (2021) 117089, https://doi.org/10.1016/j.actamat.2021.117089.
[33] H. Huang, X. Li, Z. Dong, W. Li, S. Huang, D. Meng, X. Lai, T. Liu, S. Zhu, L. Vitos, Critical stress for twinning nucleation in CrCoNi-based medium and high entropy alloys, Acta Mater. 149 (2018) 388–396, https://doi.org/10.1016/j.actamat.2018.02.037.
[34] J.W. Christian, S. Mahajan, Deformation twinning, Prog. Mater. Sci. 39 (1995) 78–84, https://doi.org/10.1002/pssb.2221910204.